Since January 2020 Elsevier has created a COVID-19 resource centre with free information in English and Mandarin on the novel coronavirus COVID-19. The COVID-19 resource centre is hosted on Elsevier Connect, the company's public news and information website.

Digital Signal Processing 127 (2022) 103577

Contents lists available at ScienceDirect

Digital Signal Processing

www.elsevier.com/locate/dsp

Parameter estimation of the COVID-19 transmission model using an improved quantum-behaved particle swarm optimization algorithm

Baoshan Ma [a,*], Jishuang Qi [a], Yiming Wu [a], Pengcheng Wang [b], Di Li [c], Shuxin Liu [d,*]

[a] School of Information Science and Technology, Dalian Maritime University, Dalian, 116026, China
[b] Department of Mechanical Engineering, University of Houston, Houston, TX, 77204, USA
[c] Department of Neuro Intervention, Dalian Medical University affiliated Dalian Municipal Central Hospital, Dalian, 116033, China
[d] Department of Nephrology, Dalian Medical University affiliated Dalian Municipal Central Hospital, Dalian, 116033, China

ARTICLE INFO

Article history:
Available online 4 May 2022

Keywords:
COVID-19
Mathematical modeling
Quantum-behaved particle swarm optimization
Parameter estimation

ABSTRACT

The outbreak of coronavirus disease (COVID-19) and its accompanying pandemic have created an unprecedented challenge worldwide. Parametric modeling and analyses of the COVID-19 play a critical role in providing vital information about the character and relevant guidance for controlling the pandemic. However, the epidemiological utility of the results obtained from the COVID-19 transmission model largely depends on accurately identifying parameters. This paper extends the susceptible-exposed-infectious-recovered (SEIR) model and proposes an improved quantum-behaved particle swarm optimization (QPSO) algorithm to estimate its parameters. A new strategy is developed to update the weighting factor of the mean best position by the reciprocal of multiplying the fitness of each best particle with the average fitness of all best particles, which can enhance the global search capacity. To increase the particle diversity, a probability function is designed to generate new particles in the updating iteration. When compared to the state-of-the-art estimation algorithms on the epidemic datasets of China, Italy and the US, the proposed method achieves good accuracy and convergence at a comparable computational complexity. The developed framework would be beneficial for experts to understand the characteristics of epidemic development and formulate epidemic prevention and control measures.

1. Introduction

Coronavirus disease (COVID-19) is defined as an infectious respiratory disease caused by Severe Acute Respiratory Syndrome Coronavirus 2 (SARS-CoV-2) [1–3]. Due to the human-to-human transmission [4], like the human influenza virus, Middle East respiratory syndrome coronavirus and SARS-CoV [5], which primarily appears through direct contact and respiratory droplets [6], the number of infections is increasing rapidly, resulting in the quick spread of COVID-19 around the world. High viral loads of SARS-CoV-2 were found in upper respiratory specimens of patients showing symptoms or asymptomatic cases, with a viral shedding pattern akin to influenza viruses [7]. Hence, the recessive transmission may play an underestimated but essential role in maintaining the epidemic. Except for the high transmission rate, the epidemic has caused enormous social and economic damage [8–11]. The World Health Organization (WHO) announced that the epidemic was a Public Health Emergency of International Concern [12–15].

Mathematical modeling of the pandemic can be used to understand the spread of the virus, predict the possible future casualties under various uncertainties and non-pharmacological policies, and provide theoretical guidance for controlling the pandemic [16–20]. The Susceptible-Infectious-Recovered (SIR) model and its extended model are widely exploited to describe the characteristics of the pandemic [21,22]. In an infectious compartmental model, $S(t)$ represents the number of susceptible cases at the time t, and new infectious cases are individuals flowing out of the S compartment. This is determined by the first derivative of $S(t)$ with respect to time, $dS(t)/dt$. The SIR model expresses this as the product of $S(t)$, $I(t)$, and a rate constant β,

$$\frac{dS(t)}{dt} = -\beta S(t) I(t), \tag{1}$$

* Corresponding authors.
E-mail addresses: mabaoshan@dlmu.edu.cn (B. Ma), root8848@sina.com (S. Liu).

https://doi.org/10.1016/j.dsp.2022.103577
1051-2004/

where $I(t)$ is the number of infectious individuals at time t.

Recently conducted researches have focused on developing various models to analyze the characteristics of COVID-19 and predict future trends, but ignored the importance of accurate parameter identification largely determining the epidemiological utility of results obtained from models. Liu et al. [23] utilized a genetic algorithm (GA) to identify the SIR model parameters and verified its effectiveness. The nonlinear least squares (LS) algorithm was presented to estimate the parameters of the proposed COVID-19 transmission model [24–29], which is a classical parameter estimation method. He et al. [30] adopted the particle swarm optimization (PSO) method to identify the SEIR model parameters in quantifying COVID-19 transmission patterns and comparing the temporal progress of disease spread in different regions. Friji et al. [31] constructed a weighted objective function and applied the Levenberg-Marquardt (LM) algorithm to optimize the parameter identification. The PSO algorithm often encounters the problem of premature convergence due to the loss of population diversity in the process of evolution, and cannot guarantee to find the global optimization in the search space [32]. The GA proposal can avoid the dilemma of local optimization to a certain extent, but it still has some limitations when facing complex problems and it is difficult to accurately converge to the global optimal solution [33]. The LM algorithm is a deterministic optimization algorithm with high computational efficiency and fast convergence, but it is sensitive to initial value selection and shows instability when minimizing the objective function. Therefore, improving the accurate parameter inference of the COVID-19 transmission model is worthy of attention.

This paper proposes an improved quantum-behaved PSO (QPSO) method to estimate the model parameters, taking advantage of the fact that these particles have quantum behavior and can appear at any position in the search space during the iteration to guarantee a robust global search ability [34]. Firstly, we develop a novel fitness function to evaluate particles and update the weighting factor of the mean best position by the reciprocal of multiplying the fitness of each best particle with the average fitness of all best particles, which can enhance the global search capacity. Secondly, we construct a probability function to generate new particles in the updating iteration to increase the variety of the population. Finally, we establish the SEAIQRD model by extending the classical SEIR model to simulate the spread of the COVID-19 pandemic. By fitting the epidemic datasets of China, Italy and the US, results indicate that the proposed method has better performance than the state-of-the-art estimation methods.

The rest of the paper is organized as follows: First, the extended SEIR model is introduced in Section 2. Then, in section 3, the novel strategies are described in the proposed algorithm. Next, the experimental results are presented in Section 4. Finally, the conclusion is drawn in Section 5.

2. The extended SEIR model

The study aims at the parameters of the COVID-19 transmission model, hence, we extend the classic SEIR model to a SEAIQRD model, accounting for the epidemiological characteristics of COVID-19 [35], which includes seven population compartments: $S(t)$ represents the susceptible individual; $E(t)$ is the exposed individual; $A(t)$ denotes the asymptomatic infection; $I(t)$ is the symptomatic infection; $Q(t)$ corresponds the confirmed individual under quarantined; $R(t)$ is the recovered case from COVID-19; $D(t)$ is the dead case from COVID-19. The following equations describe the SEAIQRD dynamical system:

$$\frac{dS(t)}{dt} = -\frac{(\alpha A(t) + \beta I(t))\, S(t)}{L}, \tag{2a}$$

$$\frac{dE(t)}{dt} = \frac{(\alpha A(t) + \beta I(t)) S(t)}{L} - \frac{E(t)}{\tau}, \tag{2b}$$

$$\frac{dA(t)}{dt} = \frac{rE(t)}{\tau} - \varepsilon A(t) - \kappa A(t), \tag{2c}$$

$$\frac{dI(t)}{dt} = \frac{(1-r)E(t)}{\tau} - \theta I(t) - \kappa I(t), \tag{2d}$$

$$\frac{dQ(t)}{dt} = \varepsilon A(t) + \theta I(t) - \eta Q(t) - \lambda Q(t), \tag{2e}$$

$$\frac{dR(t)}{dt} = \kappa (A(t) + I(t)) + \eta Q(t), \tag{2f}$$

$$\frac{dD(t)}{dt} = \lambda Q(t), \tag{2g}$$

where L denotes the population size of the region of interest, *i.e.*, $L = S + E + A + I + Q + R + D$ at each time t, and all the considered parameters are positive. The interactions between different stages are represented in Fig. 1. The parameters are defined as follows:

- α and β respectively denote the transmission rate for the asymptomatic and symptomatic cases.
- τ is the latent period.
- ε and θ denote the detection rate, relative to the asymptomatic and symptomatic cases, respectively.
- r denotes the probability of the exposed cases becoming the asymptomatic cases.
- κ and η capture the rate of recovery for the unconfirmed cases $(A(t), I(t))$ and confirmed cases, $Q(t)$.
- λ denotes the mortality rate.

The parameters of the COVID-19 transmission model are essential because they decide the spread of the epidemic and its severity [30, 36]. The values of the detection rate and the transmission rate rely on actions taken by authorities and responsible individuals before being exposed to the disease (e.g., hygiene, disinfection, quarantine, testing, social isolation, etc.) [30]. The recovery rate and the mortality rate depend on various social factors and disease (e.g., the quality and timeliness of existing health care, past health status of infected cases) [30,37]. Previous studies [24,27,30] have shown that time-varying parameters can more flexibly reflect the effect on the transmissibility

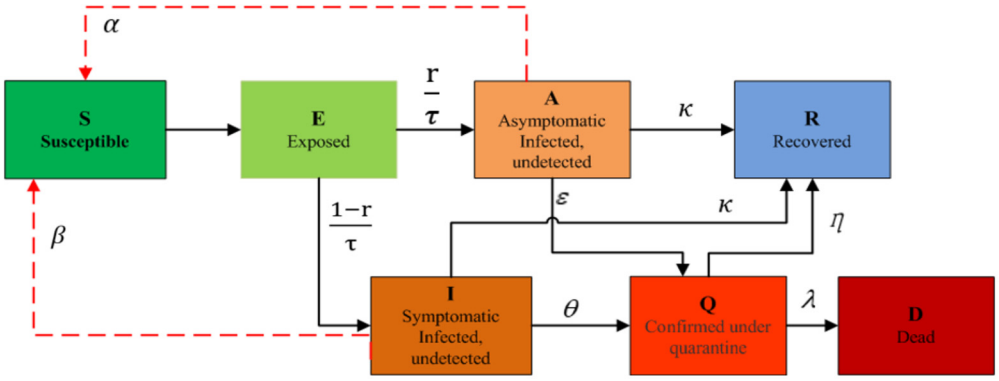

Fig. 1. The SEAIQRD model. Graphic scheme of interaction of different stages in mathematical model SEAIQRD: S, susceptible (uninfected); E, exposed; A, asymptomatic infectious (undetected); I, symptomatic infectious (undetected); Q, confirmed (under quarantine); R, recovered; D, dead.

Table 1
Major events concerning disease control.

Country	Major events	Note
China	①Jan 22 Designate 503 hospital for COVID-19 treatment ②Feb 2 Set up centralized isolation and quarantine ③Feb 16 Start nucleic acid screening	$p=3$
Italy	①Feb 1 Two cases reported ②Feb 22 Impose traffic restrictions in 11 cities ③ Mar 12 Implement "Lockdown" ④Apr 11 Launch a wider testing campaign ⑤May 18 Begin the "Second Stage" of fighting the epidemic and recovering the economy	$p=5$
The US	①Feb 1 Eight cases reported ②Mar 12 Declare a "national emergency" ③Apr 1 Issue of restrictive measures (e.g., close parks and other public places, home quarantine, facemask) ④May 1 Relax controls	$p=6$

of non-pharmaceutical interventions (NPIs) and human behavior, and more realistically simulate the evolution of the epidemic. This paper models parameters as time-varying piecewise functions. We have split the integration interval $[t_0, T]$ into p sub-intervals $[t_k, t_{k+1}]$, $k = 1, \ldots p$ (the detailed information is shown in Table 1) and parameters α, β, ε, θ, η and λ are described as follows:

$$\begin{aligned}
&\alpha(t) = \alpha_k,\\
&\beta(t) = \beta_k,\\
&\varepsilon(t) = \varepsilon_k,\\
&\theta(t) = \theta_k,\\
&\eta(t) = \eta_k,\\
&\lambda(t) = \lambda_k, \quad t \in (t_k, t_{k+1}],\ k > 0.
\end{aligned} \tag{3}$$

The SEAIQRD model is recast as follows:

$$\frac{dS(t)}{dt} = -\frac{(\alpha(t)A(t) + \beta(t)I(t))S(t)}{L}, \tag{4a}$$

$$\frac{dE(t)}{dt} = \frac{(\alpha(t)A(t) + \beta(t)I(t))S(t)}{L} - \frac{E(t)}{\tau}, \tag{4b}$$

$$\frac{dA(t)}{dt} = \frac{rE(t)}{\tau} - \varepsilon(t)A(t) - \kappa A(t), \tag{4c}$$

$$\frac{dI(t)}{dt} = \frac{(1-r)E(t)}{\tau} - \theta(t)I(t) - \kappa I(t), \tag{4d}$$

$$\frac{dQ(t)}{dt} = \varepsilon(t)A(t) + \theta(t)I(t) - \eta(t)Q(t) - \lambda(t)Q(t), \tag{4e}$$

$$\frac{dR(t)}{dt} = \kappa(A(t) + I(t)) + \eta(t)Q(t), \tag{4f}$$

$$\frac{dD(t)}{dt} = \lambda(t)Q(t). \tag{4g}$$

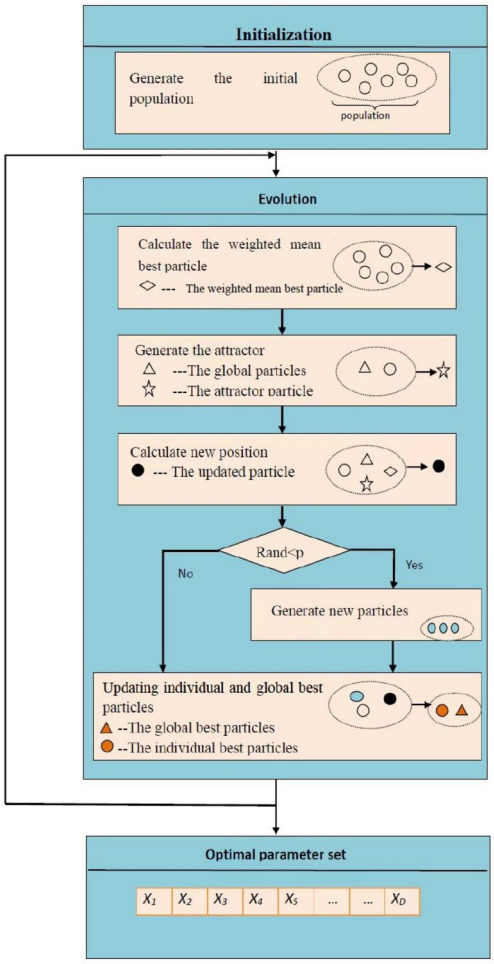

Fig. 2. The overview of the proposed algorithm.

The SEAIQRD model is an extended model that includes all the possible seven states that an individual may experience during the disease cycle and can be supported by time-varying parameters that change over time to better adapt to the variation of the pandemic data.

3. Parameter estimation method

In this section, the whole framework of the proposed algorithm is shown in Fig. 2.

3.1. The parameter estimation problem

The parameter estimation is a fitting optimization problem with three observed data inputs:

The confirmed cases under quarantined (Q): the element indicates the number of active infected cases officially reported each day.
The dead cases (D)**:** the element indicates the total number of deaths due to the COVID-19 officially reported each day.
The recovered cases (R)**:** the element indicates the total number of recovered cases officially reported each day.

We employ an improved QPSO method to solve the optimization problem, where the objective function that calculates the error between the estimated and the real data is expressed as follows:

$$f_{obj} = \frac{\sum_{n=1}^{N}(\left|\hat{Q}(n) - Q_r(n)\right| + \left|\hat{R}(n) - R_r(n)\right| + \left|\hat{D}(n) - D_r(n)\right|)}{\sum_{n=1}^{N}(Q_r(n) + R_r(n) + D_r(n))}, \tag{5}$$

where N is the number of days observed. Q_r, R_r and D_r are the observed data of infected, recovered and dead cases, respectively, $\hat{Q}$, $\hat{R}$ and $\hat{D}$ are the estimated data of infected, recovered and dead cases, respectively, provided by the SEAIQRD model.

Defining $C = [S\ E\ A\ I\ Q\ R\ D]^T$, the SEAIQRD model in Equation (3) can be recast as the following non-linear matrix form:

$$\dot{C}(t) = FC(t) + bV(t)$$

$$= \begin{bmatrix} 0 & 0 & 0 & 0 & 0 & 0 & 0 \\ 0 & -\frac{1}{\tau} & 0 & 0 & 0 & 0 & 0 \\ 0 & \frac{r}{\tau} & -(\varepsilon(t)+\kappa) & 0 & 0 & 0 & 0 \\ 0 & \frac{1-\mathrm{r}}{\tau} & 0 & -(\theta(t)+\kappa) & 0 & 0 & 0 \\ 0 & 0 & \varepsilon(t) & \theta(t) & -(\eta(t)+\lambda(t)) & 0 & 0 \\ 0 & 0 & \kappa & \kappa & \eta(t) & 0 & 0 \\ 0 & 0 & 0 & 0 & \lambda(t) & 0 & 0 \end{bmatrix} C(t)$$

$$+ \begin{bmatrix} -1 \\ 1 \\ 0 \\ 0 \\ 0 \\ 0 \\ 0 \end{bmatrix} V(t), \tag{6}$$

where

$$V(t) = S(t) \begin{bmatrix} 0 & 0 & \frac{\alpha(t)}{L} & \frac{\beta(t)}{L} & 0 & 0 & 0 \end{bmatrix} C(t). \tag{7}$$

Therefore, the parameter estimation problem of the COVID-19 transmission model is denoted as:

$$\hat{\omega} = \arg\min_{\omega} \frac{\sum_{n=1}^{N} (\left|\hat{Q}(n,\omega) - Q_r(n)\right| + \left|\hat{Q}(n,\omega) - Q_r(n)\right| + \left|\hat{Q}(n,\omega) - Q_r(n)\right|)}{\sum_{n=1}^{N} (Q_r(n) + R_r(n) + D_r(n))}, \tag{8}$$

subject to the ODE model (Eq. (9)) with initialization defined in Eq. (10).:

$$\dot{C}(n,\omega) = F \times C(n,\omega) + b \times V(n,\omega), \quad \forall n. \tag{9}$$

$$S(0) = S_0, \quad E(0) = E_0, \quad A(0) = A_0, \quad I(0) = I_0,$$

$$S(0) = S_0, \quad E(0) = E_0, \quad A(0) = A_0, \quad I(0) = I_0. \tag{10}$$

3.2. The overview of QPSO algorithm

Quantum-behaved particle swarm optimization (QPSO) algorithm is a new PSO variant, which outperforms the original PSO method on search capability but has fewer parameters to control [38]. In the QPSO algorithm, the state of a particle is depicted by a wave function, instead of its position and velocity.

By using the Monte Carlo stochastic simulation method [34], the position of the particle can be measured. The formula is as follows:

$$X_{i,j}(t+1) = \rho_{i,j}(t) \pm \frac{L_{i,j}(t)}{2} \times \ln(1/\mu), \tag{11}$$

where ρ is the attractor position and defined in Eq. (12), and μ is the random number within $(0, 1)$.

$$\rho_{i,j}(t+1) = \varphi_{i,j}(t) \times P_{i,j}(t) + \left(1 - \varphi_{i,j}(t)\right) \times G_j(t), \tag{12}$$

$P_{i,j}(t)$ represents the personal best position, $G_j(t)$ is the global best position and $\varphi_{i,j}(t)$ is the random number within $(0, 1)$.

L is defined as:

$$L_{i,j}(t) = 2\alpha \left|mbest - X_{i,j}(t)\right|, \tag{13}$$

where α is the expansion-contraction coefficient, *mbest* is the mean best position and defined as:

$$mbest = \frac{1}{M}\sum_{i=1}^{M} P_i = \left(\frac{1}{M}\sum_{i=1}^{M} P_{i1}, \frac{1}{M}\sum_{i=1}^{M} P_{i2}, \cdots, \frac{1}{M}\sum_{i=1}^{M} P_{iD}\right), \tag{14}$$

where M represents the population size and D is the dimension of the search space.

Thus, the position can be calculated by:

$$X_{i,j}(t+1) = \rho_{i,j}(t) \pm \alpha \left|mbest - X_{i,j}(t)\right| \times \ln(1/\mu). \tag{15}$$

In this paper, the QPSO algorithm is used to estimate the SEAIQRD model parameters. Specifically, the epidemic data is taken as the algorithm's input, and the output is the identified parameter. The QPSO algorithm searches for the optimal solution in the problem space through particles, and the global best position in the algorithm is the identified parameter. The pseudocode of the QPSO method for identifying SEAIQRD model parameters is given in Algorithm 1 below.

Algorithm 1 The QPSO method for identifying the SEAIQRD model parameters.

Input: the epidemic data
Output: estimated parameters: $\alpha, \beta, r, \kappa, \tau, \varepsilon, \theta, \eta, \lambda$.
initialize parameter settings and create an initial particle swarm
while termination conditions are not met **do**
Calculate $mbest(t)$.
Update $\alpha(t)$.
for $i = 1$ to N **do**
    Compute the attractor position $\rho_{i,j}(t)$
    Compute the position of the particle $X_{i,j}(t)$
    Compute the fitness of particles
    Update the individual optimal position $P_{i,j}(t)$
    Update the global optimal position $G_j(t)$
end for
end while
13: Obtain the values of the estimated parameters. The values of the global optimal position $G_j(t)$ are $\alpha, \beta, r, \kappa, \tau, \varepsilon, \theta, \eta, \lambda$.

3.3. The improved QPSO algorithm

In the original QPSO algorithm, the mean best position $mbest(t)$, guiding the direction of the population and determining the effectiveness of searching for the optimal solution, is the average of the personal best position of whole particles, regardless of the historical differences in fitness of the best position of each particle, which has difficulty in exploiting the benefit of elite particles [39]. This study designs a new strategy to update the weighted mean best position to enlarge particle search scope and vitality. In this paper, the weight is generated by the reciprocal of multiplying the fitness of each best particle with the average fitness of all best particles, and it is defined as follows:

$$w_i^t = \frac{1}{f_{obj}(P_i(t)) \cdot \frac{1}{M}\sum_{i=1}^{M} f_{obj}(P_i(t))}, \tag{16}$$

where i is the ith particle, t is the tth iteration, M represents the population size, $f_{obj}(P_i(t))$ represents the fitness of the personal best position.

$$f_{obj} = \frac{\sum_{n=1}^{N}(\left|\hat{Q}(n) - Q_r(n)\right| + \left|\hat{R}(n) - R_r(n)\right| + \left|\hat{D}(n) - D_r(n)\right|)}{\sum_{n=1}^{N}(Q_r(n) + R_r(n) + D_r(n))}, \tag{17}$$

$mbest(t)$ can be described as:

$$mbest(t) = \frac{1}{M}\sum_{i=1}^{M} w_i^t P_i = \left(\frac{1}{M}\sum_{i=1}^{M} w_{i1}^t P_{i1}, \frac{1}{M}\sum_{i=1}^{M} w_{i2}^t P_{i2}, \cdots \frac{1}{M}\sum_{i=1}^{M} w_{iD}^t P_{iD}\right). \tag{18}$$

In the QPSO algorithm, the search space of each particle in the iterative process is the whole feasible solution space of the problem. However, with the processing of evolution, the loss of population diversity is inevitable due to collectivity, just like other evolutionary algorithms based on population. Therefore, we propose a probability function to generate new particles to improve the diversity of the population. The function is described below:

$$P = e^{\left(f[G_j(t)] - \frac{1}{M}\sum_{i=1}^{M} f[X(i)]\right)/t},$$
$$\begin{cases} X_{new}(n) = rand(n, D) * (\Delta t) + boundlow, & rand < P \\ NO\ X_{new}(n), & otherwise \end{cases}, \tag{19}$$

where $f[G_j(t)]$ is the fitness of the global best position of the tth iteration, $f[X(i)]$ represents the fitness of the ith particle, P is the generation probability, M is the population size, n represents the number of new particles, Δt denotes the difference between the upper and low boundaries of the particle and *boundlow* is the low boundary, *rand* is a random number within $(0, 1)$. New particles are created when $rand < P$; otherwise, no new particles are created. This method uses Eq. (24) to evaluate the previous and new particles and updates all the particles according to the fitness.

The pseudocode of the proposed method for identifying the SEAIQRD model parameters is given in Algorithm 2 below. The accompanied code is available at: https://github.com/lab319/covid-19_model_parameters_QPSO.

4. Experimental results

To evaluate the performance of the proposed method, this study compares it with the LS, GA, PSO, QPSO, WQPSO [38] and the approach in [31]. We present the results averaged on 1000 runs and assess the metrics MAE (Mean Absolute Error), RMSE (Root Mean Squared Error), MRAE (Mean Relative Absolute Error), NRMSE (Normalized Root Mean Squared Error) and SMAPE (Symmetric Mean Absolute Percent Error), as defined in Eq. (20) to (24).

$$MAE = \frac{1}{N}\sum_{n=1}^{N}\left|y_n - \hat{y}_n\right|, \tag{20}$$

Algorithm 2 The proposed method for identifying the SEAIQRD model parameters.

Input: the epidemic data
Output: estimated parameters: $\alpha, \beta, r, \kappa, \tau, \varepsilon, \theta, \eta, \lambda$.
initialize parameter settings and create an initial particle swarm
while termination conditions are not met **do**
Compute the mean best position $mbest\,(t)$
for each particle i
Compute the attractor position using $\rho_{i,j}$.
Compute the position of the particle $X_{i,j}\,(t)$
Compute the fitness of particles
Update $P_i\,(t)\,, G(t)$.
if $rand < exp\{(f\,(gBest\,(i)) - mean(f\,(X\,(i)))/t\}$
Generate new particles: X_{new}
end if
for $z = 1 : n$
if $f(X_{new}\,(z)) < f(X\,(i))$
$X\,(i) = X_{new}\,(z)$
end if
end for
Update $P_i\,(t)\,, G(t)$.
end for
end while
Obtain the value of the estimated parameters. The value of the global optimal position $G_j\,(t)$ is the $\alpha, \beta, r, \kappa, \tau, \varepsilon, \theta, \eta, \lambda$.

Table 2
Initialization of the SEAIQRD model states for each investigated country.

Country	China	Italy	The US
N	1392730000	60430000	327000000
S_0	1392719392	60429958	326999832
E_0	5030	20	80
A_0	2515	10	40
I_0	2515	10	40
Q_0	503	2	8
R_0	28	0	0
D_0	17	0	0

Table 3
Estimated model parameters for each country.

Country	Stage	r	κ	τ	α	β	ε	θ	η	λ
China	Jan 22-Feb 1	0.102	0.128	6.050	1.855	1.861	0.020	0.045	0.015	0.014
	Feb 2-Feb 15	0.102	0.128	6.050	0.255	0.292	0.036	0.006	0.198	0.191
	Feb 16-Mar 21	0.102	0.128	6.050	0.170	0.121	0.073	0.001	0.050	0.023
	Feb 1-Feb 21	0.105	0.205	7.216	0.754	0.618	0.159	0.007	0.135	0.110
Italy	Feb 22-Mar 11	0.105	0.205	7.216	0.299	0.556	0.149	0.008	0.113	0.054
	Mar 12-Apr 10	0.105	0.205	7.216	0.227	0.237	0.014	0.010	0.138	0.145
	Apr 11-May 17	0.105	0.205	7.216	0.238	0.162	0.207	0.005	0.077	0.156
	May 18-May 30	0.105	0.205	7.216	0.133	0.085	0.039	0.002	0.134	0.098
	Feb 1-Mar 11	0.134	0.205	8.028	1.171	1.037	0.010	0.001	0.119	0.093
The US	Mar 12-Mar 31	0.134	0.205	8.028	0.586	0.549	0.010	0.004	0.001	0.101
	Apr 1-Apr 30	0.134	0.205	8.028	0.117	0.299	0.108	0.005	0.023	0.087
	May 1-May 30	0.134	0.205	8.028	0.537	0.127	0.007	0.004	0.139	0.075

Note: These values are averages on 1000 runs.

$$RMSE = \sqrt{\frac{1}{N}\sum_{n=1}^{N}\left|y_n - \hat{y}_n\right|^2}, \tag{21}$$

$$NRMSE = \frac{RMSE}{\max(y_n) - \min(y_n)}, \tag{22}$$

$$MRAE = \frac{1}{N}\sum_{n=1}^{N}\frac{\left|y_n - \hat{y}_n\right|}{\left|y_n - \overline{y}\right|}, \tag{23}$$

$$SMAPE = \frac{1}{N}\sum_{n=1}^{N}\frac{\left|y_n - \hat{y}_n\right|}{\left(\frac{y_n + \hat{y}_n}{2}\right)}, \tag{24}$$

where y_n is the observed data, $\hat{y}_n$ is the estimated data.

The initialization values of each country are given in Table 2, and the estimated parameters of the SEAIQRD model of each country are provided in Table 3. The main parameters of these comparable methods are shown in Table 4.

Table 4
Parameter setting.

Method	Parameter	Value
The proposed method and QPSO	population size	200
	iteration	1000
	dimension	p*6+3
	the expansion-contraction coefficient α	$\alpha_{max} = 1.0$, $\alpha_{min} = 0.5$
WQPSO	population size	200
	iteration	1000
	dimension	p*6+3
	the expansion-contraction coefficient α	$\alpha_{max} = 1.0$, $\alpha_{min} = 0.5$
	the weight of the mean best position ω	$\omega_{max} = 1.5$, $\omega_{min} = 0.5$
PSO	population size	200
	iteration	1000
	dimension	p*6+3
	learning factor c	$c_1 = 0.5$, $c_2 = 0.3$
	Inertial factor ω	$\omega_{max} = 0.9$, $\omega_{min} = 0.5$
GA	population size	200
	iteration	1000
	dimension	p*6+3
	mutation rate	0.1
	crossover rate	0.6

Note: p is the number of sub-interval of each country dataset, the number of time-varying parameters is 6 and the number of fixed parameters is 3.

4.1. Data source

The epidemic data was collected from authoritative and known sources as follows:

China: The dataset was collected from the statistics released by the Chinese authorities [40].

Italy and the US: The datasets were collected from the Center for Systems Science and Engineering, Johns Hopkins University [41].

Indeed, we chose Italy owing to one of the highest death rates during the first four months of the pandemic. China is one of the first affected countries witnessing the earliest but exploded in a short period. Finally, we investigate the US, which is one of the worst affected countries. For China, the data collection period, which spanned from January 22, 2020 to March 21, 2020 (the fitting period), was used to identify model parameters, and the period spanned from March 22, 2020 to April 10, 2020 was used for verification. The period spanned from February 1, 2020 to May 30, 2020 (the fitting period), in Italy and the US, was used to estimate parameters, and the period, which spanned from May 31, 2020 to June 29, 2020, was used for validation.

4.2. Fitting performance

We provide the fitting results of three countries to prove that our method can achieve accurate parameter estimation in many situations.

The fitting results of these methods on the epidemic datasets of China, Italy and the US are shown in Fig. 3, 4 and 5, respectively. In each figure, each row represents a different method, and each column is the confirmed cases, the recovered cases and the deaths, respectively. We observe that the results obtained by our method are closer to the real data; for example, in Fig. 3a the red line (the fitting data of the proposed method) is closer to the black line (real data), which indicates that the proposed method outperforms the other methods in the infected cases. Table 5 summarizes the numerical metrics of these methods for the total infected cases (the sum of the confirmed cases under quarantined Q, the recovered cases R and the Deaths D). Although the MAE and RMSE of the US epidemic dataset are higher than the other epidemic datasets because of a large number of infected cases reported, we observe that these methods show the best results on the US epidemic dataset in terms of the SAMPE and NRMSE. Notice that the MAE and RMSE of the China epidemic dataset are the smallest ones due to the low number of infected cases reported.

For the China epidemic dataset, we observe that the MAE of the proposed method shows around 950, which obtains 25%, 36%, 67%, 73%, 76%, and 62% improvements with respect to the WQPSO, QPSO, PSO, GA, LS, and the approach in [31], respectively. The MRAE of the other methods achieves 84%, 81%, 78%, 69%, 67%, and 68% less than the LS, respectively, on the Italy epidemic dataset. For the US epidemic dataset, it can be seen that the proposed method allows obtaining smaller errors than the other methods. Due to the different magnitude and trends of three observed inputs (the infected, dead and recovered cases), the algorithms may not completely fit all the curves but globally the fitting is effective as confirmed by the metrics in Table 5. In general, the proposed method provides more accurate results than other methods in these epidemic datasets.

An interesting fact can be observed in the estimation of the infected cases. The proposed method seems quite better than other methods, but for the recovered and dead cases, the performance of these methods is similar. This may be due to the developing trend of the pandemic. The cases of infection are always increasing in the US epidemic dataset, whereas there is a complex changing trend in the China and Italy epidemic datasets, specifically, the infected cases are increasing at the beginning and then decreasing. The recovered and dead cases in the three countries have a simple trend that is a slow increase. The results indicate that our method has better searching performance when dealing with complexly changing data.

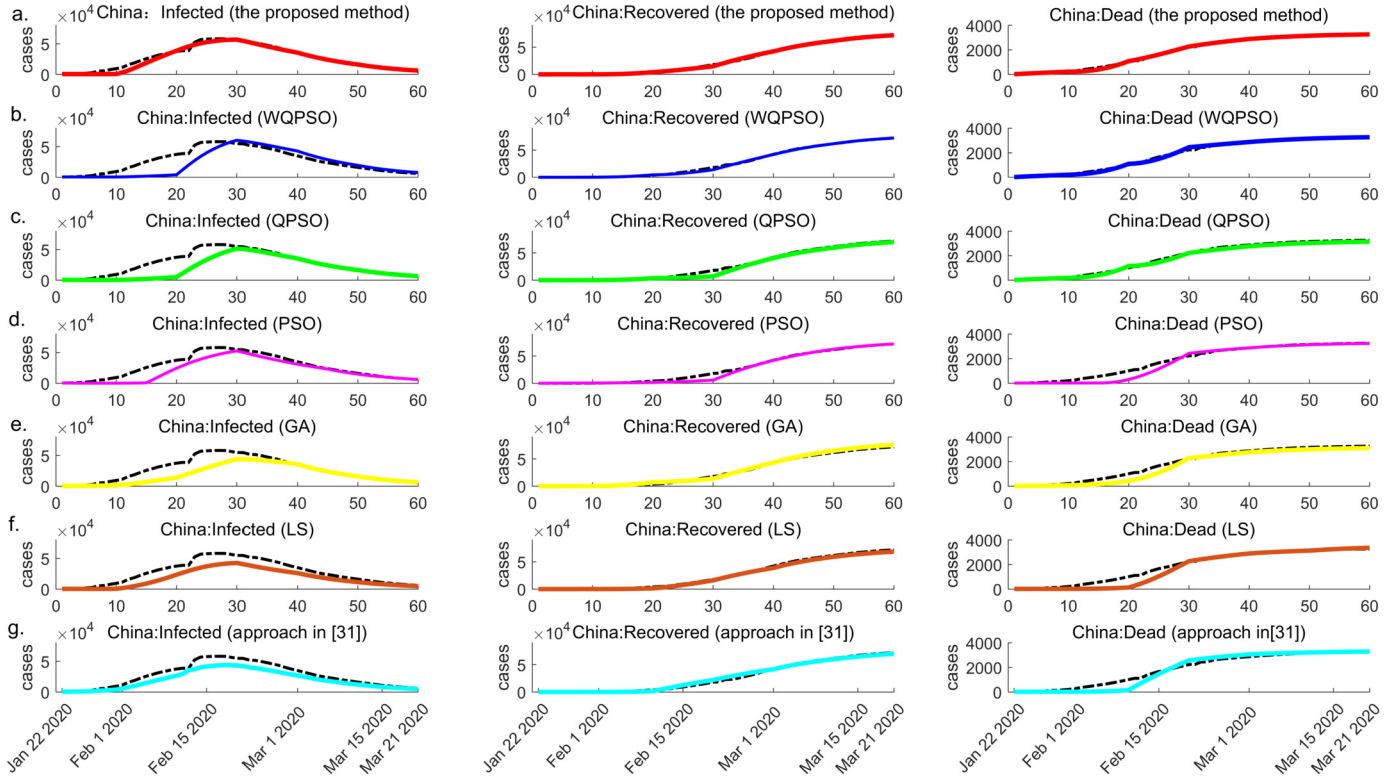

Fig. 3. China: Graphical validation of the different methods. a, the proposed method. b, WQPSO. c, QPSO. d, PSO. e, GA. f, LS. g, the approach in [31]. The colored solid line represents the model fitting results; the black dotted line represents the observed data. (For interpretation of the colors in the figure(s), the reader is referred to the web version of this article.)

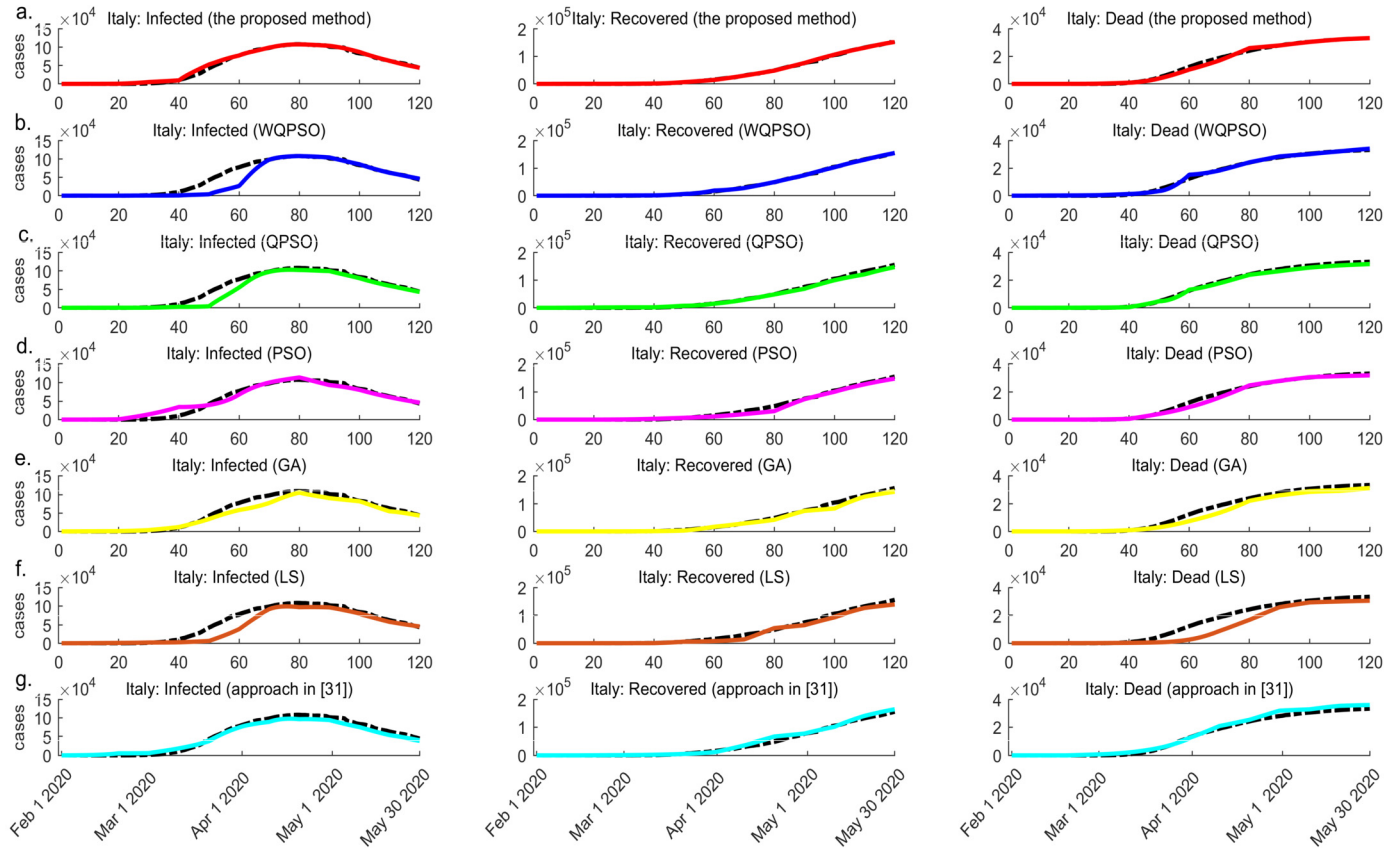

Fig. 4. Italy: Graphical validation of the different methods. a, the proposed method. b, WQPSO. c, QPSO. d, PSO. e, GA. f, LS. g, the approach in [31]. The colored solid line represents the model fitting results; the black dotted line represents the observed data.

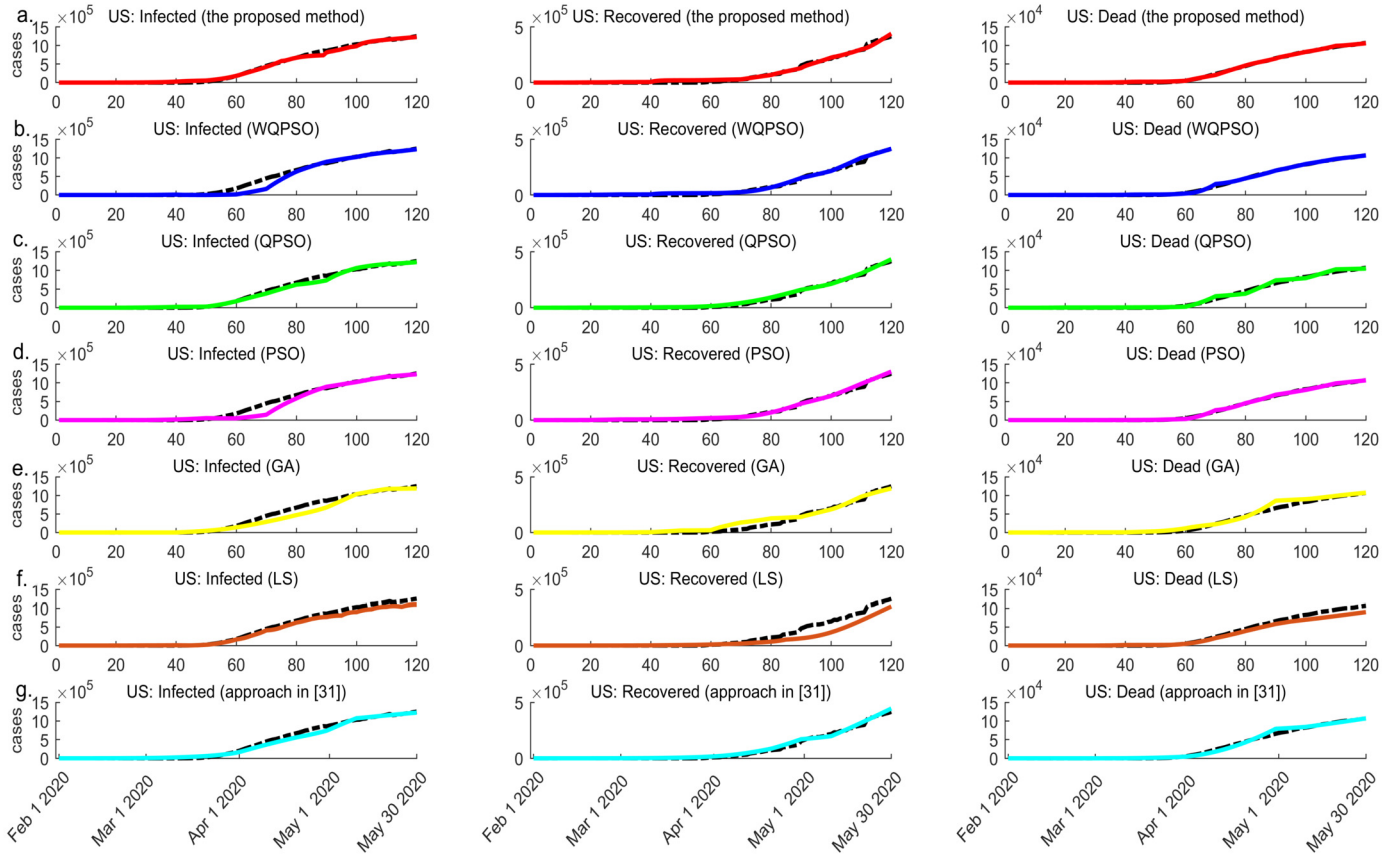

Fig. 5. The US: Graphical validation of the different methods. a, the proposed method. b, WQPSO. c, QPSO. d, PSO. e, GA. f, LS. g, the approach in [31]. The colored solid represents the model fitting results; the black dotted line represents the observed data.

Table 5
Numerical validation in the fitting period.

Data	Method	MAE	MRAE	RMSE	SMAPE	NRMSE
China epidemic dataset	The proposed method	**950.23**	**0.004**	**2155.69**	**0.254**	**0.027**
	WQPSO	1266.03	0.007	3742.87	0.340	0.046
	QPSO	1486.30	0.008	4553.81	0.501	0.056
	PSO	2920.86	0.019	5643.47	0.523	0.070
	GA	3574.17	0.020	7457.44	0.536	0.092
	LS	3907.15	0.023	8993.57	0.588	0.111
	approach in [31]	2491.53	0.015	5297.09	0.519	0.065
Italy epidemic dataset	The proposed method	**2077.62**	**0.030**	**3196.22**	**0.122**	**0.014**
	WQPSO	3161.73	0.037	6855.49	0.253	0.029
	QPSO	3465.63	0.042	7379.14	0.321	0.032
	PSO	3513.27	0.059	7522.36	0.334	0.032
	GA	4021.51	0.063	8737.88	0.374	0.038
	LS	5909.68	0.191	10238.02	0.490	0.044
	approach in [31]	3865.87	0.061	7866.79	0.354	0.034
the US epidemic dataset	The proposed method	**9817.74**	**0.028**	**21234.98**	**0.064**	**0.012**
	WQPSO	11924.43	0.043	25689.29	0.218	0.014
	QPSO	17186.66	0.081	50180.20	0.229	0.028
	PSO	18037.36	0.087	51760.26	0.251	0.029
	GA	25145.87	0.095	55870.82	0.272	0.031
	LS	27534.37	0.148	58717.91	0.283	0.034
	approach in [31]	15307.54	0.058	32877.54	0.243	0.018

Note: These metrics values are averages on 1000 runs. The best results are in bold.

4.3. Evaluation of the predictive results

In this section, the inferred models were used to predict the spread of COVID-19 in the studied countries, and these results were compared graphically and numerically to evaluate the effectiveness of the proposed method further. For China, we predicted the data for the next 20 days right after the fitting period because the epidemic was coming to an end, and for Italy and the US, we validated their prediction performance for a forecasting period of 30 days since they were still in the developing phase of the epidemic.

Table 6
Numerical validation in the predictive period.

Data	Method	MAE	MRAE	RMSE	SMAPE	NRMSE
China epidemic dataset	The proposed method	**171.45**	**0.010**	**265.23**	**0.003**	**0.176**
	WQPSO	245.81	0.011	414.58	0.006	0.275
	QPSO	395.95	0.023	449.03	0.007	0.298
	PSO	794.19	0.029	1141.63	0.021	0.758
	GA	1327.90	0.035	2065.12	0.040	1.371
	LS	1782.50	0.057	2733.53	0.064	1.815
	approach in [31]	1007.20	0.032	1183.49	0.034	0.920
Italy epidemic dataset	The proposed method	**963.33**	**0.042**	**1577.27**	**0.003**	**0.212**
	WQPSO	1655.96	0.045	1866.16	0.005	0.251
	QPSO	2872.15	0.046	3431.10	0.019	0.461
	PSO	4336.38	0.065	4864.39	0.027	0.654
	GA	5674.60	0.153	6413.81	0.037	0.862
	LS	10596.38	0.261	14104.96	0.070	1.895
	approach in [31]	4952.82	0.078	5490.84	0.031	0.738
The US epidemic dataset	The proposed method	**4229.96**	**0.051**	**4956.61**	**0.009**	**0.005**
	WQPSO	4931.05	0.053	8635.64	0.013	0.008
	QPSO	6598.04	0.068	10391.93	0.014	0.010
	PSO	7309.56	0.072	12234.56	0.016	0.011
	GA	10786.45	0.093	19832.15	0.018	0.019
	LS	76234.69	0.233	109976.84	0.162	0.102
	approach in [31]	6395.06	0.067	9575.72	0.014	0.009

We plot the forecasting results of total infected cases (the sum of the confirmed cases under quarantined Q, the recovered cases R, and the deaths D) in Fig. 6 and the result of each case is provided in Supplementary Figure S1. At the fitting period, these methods perform, approximately, the same level of efficiency (Fig. 3–5). On the contrary, at the predictive stage, it can be observed that our method outperforms other methods (in Fig. 6). In fact, the curve generated from the model inferred by our method is the closest to the real value, suggesting that the proposed method yields higher accuracy than the other existing estimation methods in these epidemic datasets.

The numerical results in Table 6 prove the outperformance of the proposed method compared to the other methods in the studied countries. In the US epidemic dataset, the RMSE of our method achieves 43%, 52%, 59%, 75%, 95%, and 48% less than the WQPSO, QPSO, PSO, GA, LS, and the approach in [31], respectively. The SMAPE of the proposed method, WQPSO, QPSO, PSO, GA, and the approach in [31] yield 95%, 91%, 89%, 67%, 38%, and 48% less than the LS, respectively, in the China epidemic dataset. For the NRMSE using the Italy epidemic dataset, our method shows 16%, 54%, 68%, 75%, 89%, and 71% less than the other methods, respectively. Similar observations are noticed of other metrics as well.

From Fig. 6, we observe that only the Italian data is overestimated. Actually, the initial value of the prediction stage is the value of the last point in the fitting stage. The deviation between the estimated value and the observed value in the later fitting stage will lead to a biased prediction result.

4.4. Convergence

To evaluate the convergence of these methods, this study presents the comparison of convergence averaged on 1000 runs when the maximum generation is 1000 and the population size is 200. The measurement was conducted on a computer with Intel(R) Core (TM) CPU i5-9300H, clocked at 2.4 GHz and 8 GB memory. The minor, mean and variance of the fitness for each method are provided in Table S1 (the supplemental material). Fig. 7 shows the convergence curves of these methods. The result shows that the MSE of each method decreases gradually with the increase of the iteration number and the LS and PSO methods converge faster. When the iteration is about 400 the proposed method tends to be stable and has the smallest errors.

4.5. Computation complexity

In each generation, the proposed method performs the following four operations:

(1) updating the particles
(2) calculating the fitness of the particles
(3) generating new particles and calculating the fitness
(4) updating the personal best position and the global best position

In the proposed method, given the population size M and dimension size D, the computational complexity for updating the particles and calculating the fitness of all particles is $O(2^*M^*D)$. To increase the diversity of the population, n new particles would be generated ($n < M$), which needs a runtime of $O(n^*D)$ and the complexity for calculating its fitness is $O(n^*D)$. Updating the personal best position and the global best position costs a runtime of $O(M^*D)$. Based on the above analyses, the overall computational complexity of the proposed method is $O(P^*(M + n)^*D)$, where P is the total number of generations. Table 7 gives an overview of the average running time of each method. The comprehensive complexity analyses of the other methods are provided in the supplemental material. We observe that the LS and the approach in [31] run faster, but the proposed method does not show a significant disparity with the other four methods.

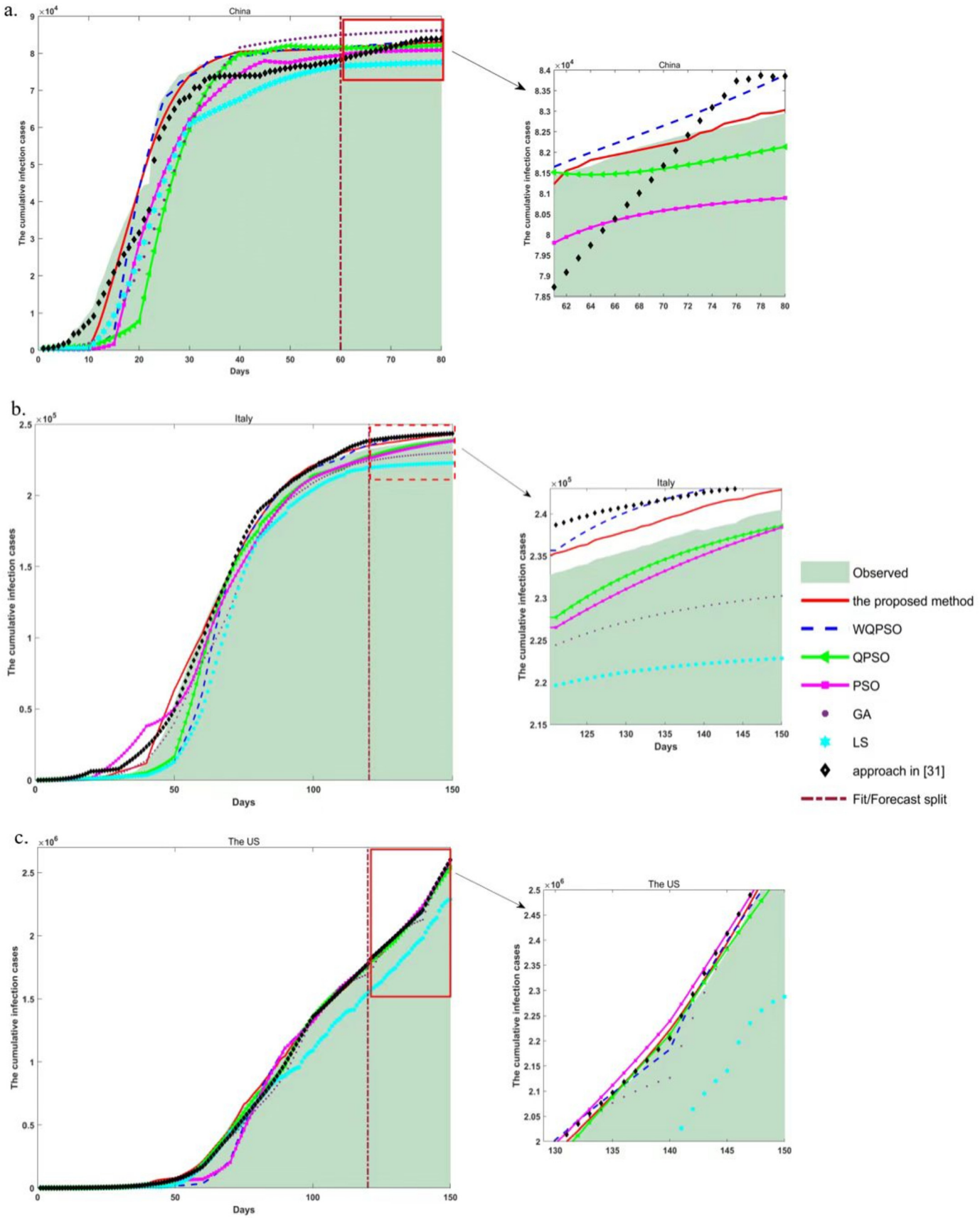

Fig. 6. Comparative analysis of the prediction results. The ordinate is the number of cumulative infection case, it consists of the active confirmed cases (Q), the recovered cases (R) and the deaths (D). The abscissa is the number of days. **a**. China epidemic dataset; **b**. Italy epidemic dataset; **c**. the US epidemic dataset.

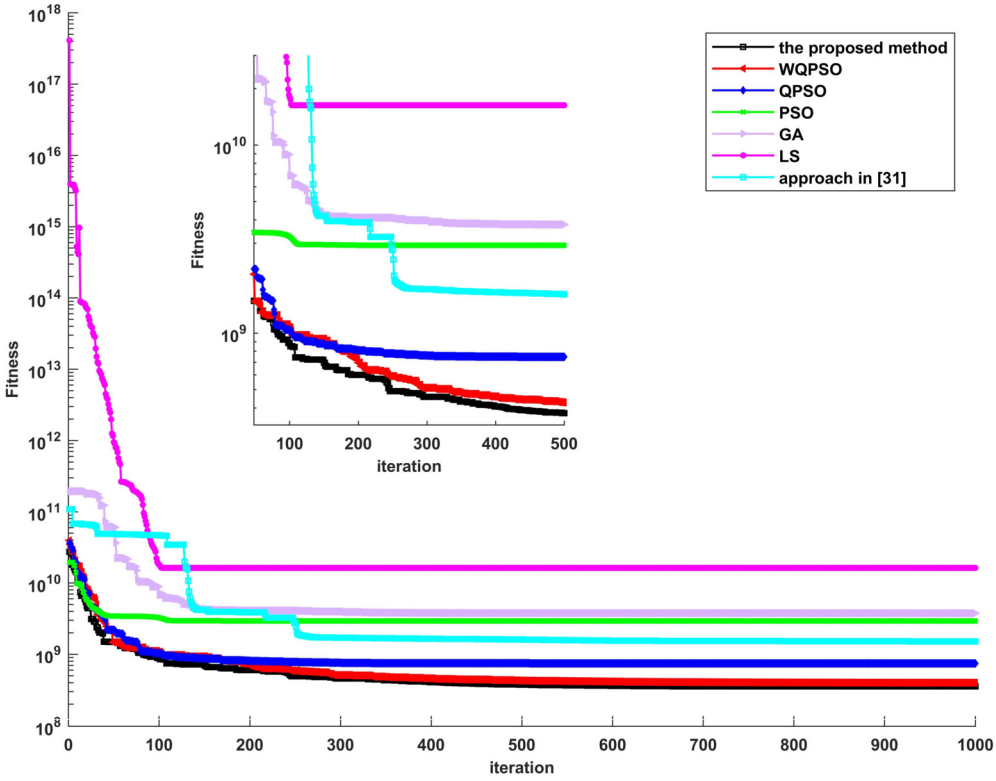

Fig. 7. Comparison of the convergence.

Table 7
The average runtime time of each method.

Method	Complexity	China epidemic dataset	Italy epidemic dataset	The US epidemic dataset
The proposed method	$O(P^*(M+n)^*D)$	220.5 s	364.6 s	371.7 s
WQPSO	$O(P^*M\ ^*D)$	150.8 s	250.7 s	291.9 s
QPSO	$O(P^*M\ ^*D)$	140.1 s	238.4 s	285.3 s
PSO	$O(P^*M\ ^*D)$	113.7 s	237.5 s	269.8 s
GA	$O(P^*M\ ^*D^2)$	341.2 s	647.5 s	676.7 s
LS	$O(P)$	3.6 s	40.5 s	67.3 s
Approach in [31]	$O(P)$	7.5 s	69.5 s	93.5 s

4.6. Discussion

In the paper, we propose an improved quantum-behaved particle swarm optimization (QPSO) algorithm to estimate the parameters of the SEAIQRD model. First, we develop a new strategy to update the weighting factor of the mean best position, which can enhance the global search capacity. Second, we design a probability function for generating new particles in the updating iteration to increase the particle diversity. We perform 1000 repetitions of each algorithm on China, Italy and the US epidemic datasets, and use metrics MAE, RMSE, MRAE, RMSPE and SMAPE to evaluate the performance of the algorithms. From the experimental results, we observe that the proposed algorithm achieves the lowest errors due to the advantage of our method in searching optimal solution. The results also show that the proposed algorithm is effective.

In order to further verify the validity of these two new strategies of the proposed method, the comparison between the algorithm using only one strategy and other algorithms is given in the supplement material Table S2. For the China epidemic dataset, we observe the MAE of the method only using probability function is around 1017, which obtains 20%, 17%, 74%, and 59% improvements than the WQPSO, QPSO, PSO, GA, LS, and the approach in [31], respectively. Similar observations are noticed of the other datasets as well. The results suggest the effectiveness of the probability function in improving the search capacity. In the Italy epidemic dataset, the RMSE of the method only using the weighted mean best position achieves a 9%, 16%, 17%, 29%, 39%, and 21% less than the WQPSO, QPSO, PSO, GA, LS, and the approach in [31], respectively. The numerical results show the outperformance of the method only using the weighted mean best position in enhancing the global search capacity.

From Table 3, we observe that the transmission rates α and β substantially decrease from 1.855 and 1.861 in the first period to 0.255 and 0.292, 0.170 and 0.121 in the latter two periods after a series of multifaceted public health interventions in China. From the results of Italy, the mortality rate λ remains high in the first four periods and decreased to 0.098 in the fifth stage. The transmission rates α and β of the US are relatively large during the four periods despite a series of interventions, and the epidemic would not calm down in a short time. The three countries are representative and can provide theoretical guidance for other countries in the world to control the

pandemic. In addition, we provided code of the proposed algorithm that researchers can use to evaluate the epidemic in the interested countries (https://github.com/lab319/covid-19_model_parameters_QPSO).

Finally, to assess the statistical significance of the differences between the different algorithms, we plot a boxplot (in the supplement material Figure S2) to show the results (NRMSE) of 1000 replicates of each algorithm. We observe that the mean and variance of the proposed method are the lowest, which indicates that our method is more stable and accurate, and our method has a significant statistical difference from the other methods (t-test, $p < 0.05$).

5. Conclusion

This paper proposes an improved QPSO method to estimate the parameters of the SEAIQRD model. The established SEAIQRD can be supported by the time-varying parameters that change over time to better adapt to the variations of the pandemic. The novelties of the proposed method are that the fitness of particles is regarded as the weight of the mean best position to enhance the global search capacity, and the probability function is constructed for generating new particles to increase the diversity of the population. Further, the estimated cases of infected, recovered and dead using the inferred SEAIQRD model have been compared with the actual epidemic data in China, Italy and the US. The experimental results demonstrate that the proposed method achieves good accuracy and convergence at a comparable computational complexity. In future work, we will further focus on finding a more effective control method to improve the performance of the QPSO algorithm.

CRediT authorship contribution statement

Baoshan Ma: Conceptualization, Supervision, Writing – review & editing. **Jishuang Qi:** Conceptualization, Data curation, Investigation, Software, Writing – original draft, Writing – review & editing. **Yiming Wu:** Software, Writing – review & editing. **Pengcheng Wang:** Data curation, Writing – review & editing. **Di Li:** Data curation, Writing – review & editing. **Shuxin Liu:** Conceptualization, Supervision, Writing – review & editing.

Declaration of competing interest

The authors declare that they have no known competing financial interests or personal relationships that could have appeared to influence the work reported in this paper.

Acknowledgments

This work was supported by the National Natural Science Foundation of China under Grant 61471078.

Appendix A. Supplementary material

Supplementary material related to this article can be found online at https://doi.org/10.1016/j.dsp.2022.103577.

References

[1] M. Chinazzi, J.T. Davis, M. Ajelli, et al., The effect of travel restrictions on the spread of the 2019 novel coronavirus (COVID-19) outbreak, Science 368 (6489) (2020) 395–400.
[2] W. Souza, L.F. Buss, D. Candido, et al., Epidemiological and clinical characteristics of the COVID-19 epidemic in Brazil, Nat. Hum. Behav. 4 (8) (2020) 856–895.
[3] Y.N. Kyrychko, K. Blyuss, I. Brovchenko, Mathematical modelling of the dynamics and containment of COVID-19 in Ukraine, Sci. Rep. 19662 (2020) (2020) 1–11.
[4] X. Hao, S. Cheng, D. Wu, et al., Reconstruction of the full transmission dynamics of COVID-19 in Wuhan, Nature 584 (2020) (2020) 1–7.
[5] W.J. Guan, Z.Y. Ni, Y. Hu, et al., Clinical characteristics of coronavirus disease 2019 in China, J. Integr. Med. 58 (4) (2020) 395–400.
[6] M. Peirlinck, F.S. Costabal, K. Linka, et al., Outbreak dynamics of COVID-19 in China and the United States, Biomech. Model. Mechanobiol. 19 (2020) (2020) 2179–2193.
[7] J. Ren, Y. Yan, H. Zhao, et al., A novel intelligent computational approach to model epidemiological trends and assess the impact of non-pharmacological interventions for COVID-19, IEEE J. Biomed. Health Inform. 24 (12) (2020) 3551–3563.
[8] J.T. Wu, L. Kathy, G.M. Leung, Nowcasting and forecasting the potential domestic and international spread of the 2019-nCoV outbreak originating in Wuhan, China: a modelling study, Lancet 395 (10225) (2020) 689–697.
[9] F. Song, N. Shi, F. Shan, et al., Emerging 2019 novel coronavirus (2019-nCoV) pneumonia, Radiology 297 (3) (2020) 346–352.
[10] V. Chamola, V. Hassija, V. Gupta, et al., A comprehensive review of the COVID-19 pandemic and the role of IoT, drones, AI, blockchain and 5G in managing its impact, IEEE Access 8 (2020) 90225–90265.
[11] K.M. Bubar, S.M. Kissler, M. Lipsitch, et al., Model-informed COVID-19 vaccine prioritization strategies by age and serostatus, Science 371 (6532) (2020) 916–921.
[12] Y.P. Tan, B.Y. Tan, J. Pan, et al., Epidemiologic and clinical characteristics of 10 children with coronavirus disease 2019 in Changsha, China, J. Clin. Virol. 127 (104353) (2020) 1–6.
[13] J. Bedford, D. Enria, J. Giesecke, et al., COVID-19: towards controlling of a pandemic, Lancet 395 (10229) (2020) 1–4.
[14] World Health Organization (WHO), The WHO characterizes the COVID-119 as a pandemic [Online]. Available: https://www.who.int/emergencies/diseases/novel-coronavirus-2019/events-as-they-happen, Jul. 1, 2020.
[15] O.P. Neto, D.M. Kennedy, J.C. Reis, et al., Mathematical model of COVID-19 intervention scenarios for So Paulo—Brazil, Nat. Commun. 12 (418) (2021) 1–13.
[16] A.J. Kucharski, T.W. Russell, C. Diamond, et al., Early dynamics of transmission and control of COVID-19: a mathematical modelling study, Lancet Infect. Dis. 20 (5) (2020) 553–558.
[17] K. Prem, Y. Liu, T.W. Russell, The effect of control strategies to reduce social mixing on outcomes of the COVID-19 epidemic in Wuhan, China: a modelling study, Lancet Public Health 5 (5) (2020) 261–270.
[18] G. Giordano, F. Blanchini, R. Bruno, et al., Modelling the COVID-19 epidemic and implementation of population-wide interventions in Italy, Nat. Med. 26 (2020) (2020) 855–860.
[19] C. Anastassopoulou, L. Russo, A. Tsakris, et al., Data-based analysis, modelling and forecasting of the COVID-19 outbreak, PLoS ONE 15 (3) (2020) 1–21.
[20] S. Khoshnaw, R. Salih, S. Sulaimany, Mathematical modelling for coronavirus disease (COVID-19) in predicting future behaviours and sensitivity analysis, Math. Model. Nat. Phenom. 15 (33) (2020) 1–16.
[21] C. Huang, Y. Wang, X. Li, et al., Clinical features of patients infected with 2019 novel coronavirus in Wuhan, China, Lancet 395 (10223) (2020) 497–506.

[22] Z. Yang, Z. Zeng, K. Wang, et al., Modified SEIR and AI prediction of the epidemics trend of COVID-19 in China under public health interventions, J. Thorac. Dis. 12 (3) (2020) 165–174.
[23] S. Liu, Application of genetic algorithm to SIR model parameters, J. Geomat. 37 (6) (2012) 6–9.
[24] M. Bahloul, A. Chahid, T.M. Laleglkirati, Fractional-order SEIQRDP model for simulating the dynamics of COVID-19 epidemic, IEEE Open J. Eng. Med. Biol. 1 (2020) 249–256.
[25] C. Tsay, F. Lejarza, M.A. Stadtherr, et al., Modeling, state estimation, and optimal control for the US COVID-19 outbreak, Sci. Rep. 10 (1) (2020) 1–12.
[26] L. López, X. Rodó, The end of social confinement and COVID-19 re-emergence risk, Nat. Hum. Behav. 4 (7) (2020) 746–755.
[27] E.L. Piccolomini, F. Zama, Monitoring Italian COVID-19 spread by an adaptive SEIRD model, PLoS ONE 15 (8) (2020) 1–17.
[28] O. Tustoy, K. Balikci, N.F. Ozdil, Unknown uncertainties in the COVID-19 pandemic: multi-dimensional identification and mathematical modelling for the analysis and estimation of the casualties, Digit. Signal Process. 114 (5) (2021) 1–10.
[29] G.L. Watson, D. Xiong, L. Zhang, et al., Pandemic velocity: forecasting COVID-19 in the US with a machine learning & Bayesian time series compartmental model, PLoS Comput. Biol. 17 (3) (2021) 1–20.
[30] J. He, G. Chen, Y. Jiang, et al., Comparative infection modeling and control of COVID-19 transmission patterns in China, South Korea, Italy and Iran, Sci. Total Environ. 747 (141447) (2020) 1–15.
[31] H. Friji, R. Hamadi, H. Ghazzai, et al., A generalized mechanistic model for assessing and forecasting the spread of the COVID-19 pandemic, IEEE Access 9 (2021) 13266–13285.
[32] A. Ratnaweer, S.K. Halgamuge, H.C. Watson, Self-organizing hierarchical particle swarm optimizer with time-varying acceleration coefficients, IEEE Trans. Evol. Comput. 8 (3) (2004) 240–255.
[33] J. Li, L. Li, A hybrid genetic algorithm based on information entropy and game theory, IEEE Access 8 (2020) 36602–36611.
[34] J. Sun, B. Feng, W. Xu, Particle swarm optimization with particles having quantum behavior, in: Proc. Congr. Evol. Comput, vol. 1, 2004, pp. 325–331.
[35] H. Nishiura, T. Kobayashi, A. Suzuki, et al., Estimation of the asymptomatic ratio of novel coronavirus infections (COVID-19), Int. J. Infect. Dis. 94 (3) (2020) 154–155.
[36] H. Khataee, I. Scheuring, A. Czirók, et al., Effects of social distancing on the spreading of COVID-19 inferred from mobile phone data, Sci. Rep. 11 (1661) (2021) 1–9.
[37] H. Rossman, T. Meir, J. Somer, et al., Hospital load and increased COVID-19 related mortality in Israel, Nat. Commun. 12 (1904) (2021) 1–7.
[38] M. Xi, J. Sun, W. Xu, An improved quantum-behaved particle swarm optimization algorithm with weighted mean best position, Appl. Math. Comput. 205 (2) (2008) 751–759.
[39] J. Yi, J. Bai, W. Zhou, et al., Operating parameters optimization for the aluminum electrolysis process using an improved quantum-behaved particle swarm algorithm, IEEE Trans. Ind. Inform. 14 (8) (2017) 3405–3414.
[40] National Health Commission of the People's Republic of China (NHC) [Online]. Available: http://www.nhc.gov.cn/xcs/yqtb/list_gzbd.shtml. (Accessed 28 March 2020).
[41] Johns Hopkins University Center for Systems Science and Engineering [Online]. Available: https://coronavirus.jhu.edu/.

Baoshan Ma received the B.S. degree in mechatronics engineering from the Harbin Engineering University, Harbin, China, in 2000, the Ph.D. degree in communication and information system from the Dalian Maritime University, Dalian, China, in 2008. He is currently an Associate Professor with the School of Information Science and Technology, and is also affiliated with the Institute of Environmental Systems Biology, Dalian Maritime University. His research interests include signal processing, machine learning and bioinformatics.

Jishuang Qi received the B.S. degree in communication engineering from Taishan University, Taian, Shandong, China, in 2019 and she is currently pursuing the M.S. degree in information and communication engineering at Dalian Maritime University, Dalian, China. Her research interests include signal processing, computational biology and bioinformatics.

Yiming Wu received the B.S. degree in electronic information engineering from Civil Aviation University of China, Tianjian, Chian, in 2020, and he is currently pursuing the M.S. degree in information and communication engineering at Dalian Maritime University, Dalian, China. His research interests include gene regulatory networks and machine learning algorithms based on gene expression data analysis.

Pengcheng Wang received B.S. in Marine Engineering and M.S. in Naval Architecture and Ocean Engineering from Dalian Maritime University. He also received M.S. in Industrial Engineering from the University of Houston in 2019. He is currently a Ph.D. student majoring in Mechanical Engineering at the Cullen College of Engineering, University of Houston. His research interests include Machine Learning, the fracturing process of metamaterials, and electrical signals of metamaterials.

Di Li received the Ph.D. and M.D. degree in Beijing Neurosurgical Institute affiliated Capital Medical University, in 2016. He is currently the director of Neurointerventional and Neurocritical care department, Dalian Central Hospital affiliated Dalian Medical University, China. His research interests include stroke, severe pneumonia and epidemiology of cerebrovascular disease.

Shuxin Liu received the Ph.D. and M.D. degree in Chinese People's Liberation Army General Hospital, in 2007. She is currently the director of Nephropathy and Hemodialysis Department, Dalian Central Hospital affiliated Dalian Medical University, China. Her research interests include glomerulonephritis, hemodialysis and epidemiology of chronic kidney disease.